ELSEVIER

Polymer 44 (2003) 2975–2982

polymer

www.elsevier.com/locate/polymer

Analysis of gas transport properties of PPO/PS blends by ^{129}Xe NMR spectroscopy

Tomoyuki Suzuki, Hiroaki Yoshimizu*, Yoshiharu Tsujita

Polymeric Materials Course, Department of Materials Science and Engineering, Nagoya Institute of Technology, Gokiso-cho, Showa-ku, Nagoya 466-8555, Japan

Received 14 November 2002; received in revised form 10 February 2003; accepted 20 February 2003

Abstract

Relationships among variations of microvoids and gas transport properties for miscible poly(2,6-dimethyl-1,4-phenylene oxide) (PPO)/polystyrene (PS) blends in the glassy state have been investigated by Xe sorption, Xe permeation, and ^{129}Xe NMR measurements. Xe sorption isotherms of the blends can be interpreted successfully on the basis of the dual-mode sorption model. Decrease in the permeability of Xe is attributed to the decrease in the diffusivity of that in the Langmuir site. ^{129}Xe NMR spectra of ^{129}Xe in the blends show non-linear low-field shift with increasing sorption amount of Xe because of a fast exchange of Xe atoms between Henry and Langmuir sites. From the analysis of ^{129}Xe NMR chemical shifts, it is found that the mean volume of individual microvoids varies with a negative deviation against volume fraction of PPO in the blend. For PPO/PS blends, it has been clarified that the contraction of individual microvoids occurs by blending and highly affects gas transport properties.

Keywords: ^{129}Xe NMR; Gas transport properties; Microvoids

1. Introduction

Microvoids are formed in a dense polymer matrix as interspaces among molecular chains when the polymer becomes glassy state and its segmental mobility of main chains is frozen [1–3]. It is important to characterize microvoids because they highly affect mechanical and gas transport properties of glassy polymers [4–6]. Fig. 1 shows the schematic diagram of a conventional specific volume–temperature curve. Total amount of microvoids is corresponding to the unrelaxed-volume region as shown in Fig. 1. Generally, evaluations of gas sorption properties of a glassy polymer can provide some information about unrelaxed-volume or microvoids. Gas sorption behavior of a glassy polymer can be interpreted by the dual-mode sorption model [1–7], which is represented by following equation:

$$C = C_D + C_H = k_D p + \frac{C'_H b p}{1 + bp} \quad (1)$$

where C is the equilibrium sorption amount at pressure p, C_D is the concentration of the penetrant due to the Henry's law contribution, C_H is that held in the Langmuir site, k_D is the solubility coefficient of Henry's law, b is the affinity constant of the Langmuir site, and C'_H is the Langmuir saturation constant. Langmuir-mode sorption is interpreted by the sorption into microvoids of a glassy polymer [8–10]. Hence, one can obtain prime information about microvoids from evaluations of C_H and parameter C'_H.

In recent years, ^{129}Xe NMR spectroscopy has become a powerful technique of materials characterization. Since Xe atom has a very large polarizability, ^{129}Xe NMR signal of ^{129}Xe sorbed in a medium is sensitively affected by surrounding environments. For micro porous materials like zeolites, the NMR chemical shift of adsorbed ^{129}Xe is explained by the following equation [11–17]:

$$\delta = \delta(S) + \delta(Xe) + \delta(E) + \delta(SAS) + \delta(M) \quad (2)$$

δ is the observed NMR chemical shift of adsorbed ^{129}Xe. δ(S) is the chemical shift due to interaction between Xe and inner wall of hole. δ(Xe) corresponds to the interaction between Xe atoms and increases in proportion to

* Corresponding author. Tel./fax: +81-52-735-5272.
E-mail address: yosimizu@mse.nitech.ac.jp (H. Yoshimizu).

0032-3861/03/$ - see front matter © 2003 Elsevier Science Ltd. All rights reserved.
doi:10.1016/S0032-3861(03)00191-5

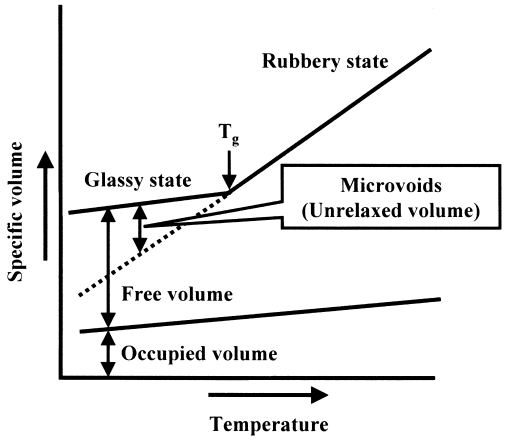

Fig. 1. Schematic diagram of the specific volume–temperature curve.

concentration of Xe. δ(E), δ(SAS), and δ(M) are terms explained by the contribution of the electric field created by multivalent cations, the interaction of Xe with the strong adsorption site, and the contribution of the magnetic field created by paramagnetic compensation cations, respectively [15–17]. However, the contributions of δ(E), δ(SAS), and δ(M) can be ignored for most of the polymers because of absence of strong charge groups. Observed δ for a polymer, therefore, can be explained as a sum of δ(S) and δ(Xe).

For the studies of zeolites, there have been many reports that δ(S) value is strongly correlated with the size of a hole in which Xe atom is sorbed [11–14,18–21]. For polymer systems, in addition, some researches have also been reported about the relation between ^{129}Xe NMR chemical shift and size of hole that gives free volume or microvoids [22–28]. In our previous studies, we have reported that ^{129}Xe NMR chemical shifts for glassy polymers show non-linear low-field shift with increasing sorption amount of Xe because of a fast exchange of Xe between Henry- and Langmuir-mode sorption sites, and we have consequently enabled to evaluate mean size of microvoids in glassy polymers [29–31]. As another technique, positron annihilation lifetime spectroscopy (PALS) is useful to investigate size and distribution of free volume in polymers [32–38]. However, the PALS technique cannot estimate microvoids in glassy polymers independently.

In this study, relationships among variations of microvoids and Xe transport properties for miscible poly(2,6-dimethyl-1,4-phenylene oxide) (PPO)/polystyrene (PS) blends are investigated by Xe sorption, Xe permeation, and ^{129}Xe NMR measurements. PPO/PS blend system is one of the well-known miscible blends and is in glassy state at room temperature [39]. Using the blend system, it becomes easy to control contents of microvoids and will be able to evaluate the correlation between ^{129}Xe NMR chemical shift and size of microvoids in detail.

2. Experimental

2.1. Sample preparations

Sample membranes (PPO/PS = 0/100, 20/80, 50/50, 80/20, 100/0) were prepared by a solution-casting method with chloroform as co-solvent of PPO and PS. Each membrane was annealed above the glass transition temperature (T_g) for 3 h, and then cooled slowly. Density of a membrane was measured by a flotation method with NaBr aqueous solution at 25 °C.

2.2. Xe sorption measurements

Xe sorption measurements were carried out using a gravimetric sorption apparatus with an electro-microbalance (CAHN 2000, Cahn Instruments, Inc.) at 25 °C. After sufficient evacuation of a membrane, required pressure of Xe was introduced in the apparatus. Sorption amount of Xe for the membrane was determined after correction of the contribution of buoyancy.

2.3. Xe permeation measurements

Xe permeation measurements were carried out using a hand-made permeation apparatus employed in our laboratory. A membrane, which was held in the permeation cell sealed with O-rings, was evacuated for 24 h or more in the permeation apparatus. A desired pressure of Xe was introduced on the upstream side, and downstream side of the membrane was held at high vacuum. The pressure on the upstream side was monitored using Baratron127AA pressure transducer (MKS Instruments, Inc.). Permeability coefficient was obtained from the permeation rate that was monitored as the variation of pressure on the downstream side at steady state using another Baratron127AA pressure transducer.

2.4. ^{129}Xe NMR measurements

Cut membrane was packed about 1 g into a 10 mmϕ Pyrex NMR sample tube with thick wall (Type 513-7 JYH-7, Wilmad), and degassed for 24 h. After that, required amount of Xe (with natural abundance of ^{129}Xe) was introduced into the NMR tube with the aid of liquid nitrogen, and the tube was sealed with Teflon valve. Internal pressure was determined from sorption amount of Xe for the membrane and total weight of Xe in the NMR tube. ^{129}Xe NMR spectra were recorded on a JEOL GX400 NMR spectrometer at 110.5 MHz and 25 °C. All of ^{129}Xe NMR chemical shifts were referred to an external standard of ^{129}Xe in gas phase at zero-pressure as 0 ppm.

3. Results and discussion

3.1. Xe transport properties of PPO/PS blends

Fig. 2 shows the composition dependence of the specific volume, V_m, determined from the density measurement. It is obviously confirmed that V_m values of the blends are lower than those calculated by following additive rule

$$V_m = w_{PS}V_{PS} + w_{PPO}V_{PPO} \quad (3)$$

$$w_{PS} + w_{PPO} = 1 \quad (4)$$

w_{PS} and w_{PPO} are weight fractions of PS and PPO in the blend, respectively. V_{PS} and V_{PPO} are specific volumes of pure PS and PPO, respectively. From Fig. 2, therefore, it can be said that a volume contraction is taken place by blending for PPO/PS blends, which may be attributed to an attractive interaction between methyl groups of PPO and phenyl rings of PS [39].

Xe sorption isotherms of the blends are shown in Fig. 3. It is clear that these isotherms are concave toward the pressure axis. These isotherms could be explained successfully on the basis of the dual-mode sorption model (Eq. (1)), and the results of curve fitting are drawn in Fig. 3 as solid lines. The dual-mode sorption parameters were determined by a non-linear least-square method and summarized in Table 1 together with T_g of the blend. C'_H is one of the indicators of total amount of microvoids in a glassy polymer, and plotted against volume fraction of PPO in the blend as shown in Fig. 4. It appears that obtained $C_{H'}$ is smaller than that expected from a simple additive rule drawn as dashed line, whereas k_D and b follow additive rules, respectively. This fact indicates that the decrease in the total amount of microvoids in the blends has occurred by blending, which is consistent with the result of the density measurement.

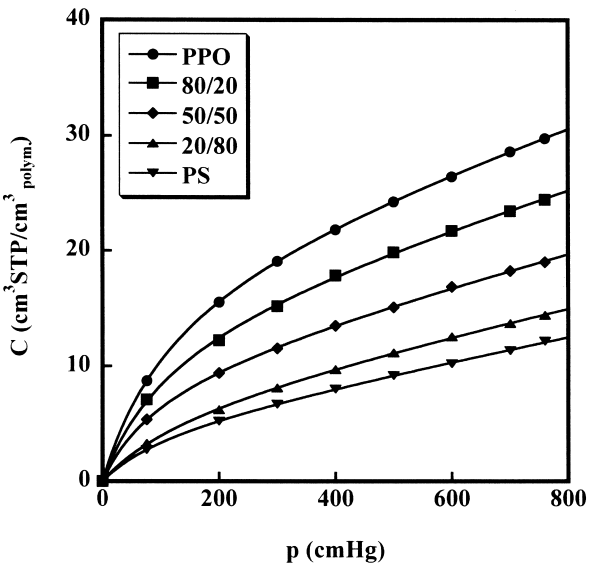

Fig. 3. Xe sorption isotherms of PPO/PS blends at 25 °C.

Xe permeability coefficients for the blends at 76 cmHg are shown in Fig. 5(a). It appears that permeability coefficients for the blends are lower than those expected from a semilogarithmic additive rule. In general, gas transport properties of a polymer can be explained on the basis of the solution-diffusion mechanism, which is represented by following equations [40–43]:

$$\bar{P} = S \times \bar{D} \quad (5)$$

$$S = \frac{C}{p} \quad (6)$$

where $\bar{P}$, S, and $\bar{D}$ are permeability, solubility, and diffusion coefficients, respectively. The S can be calculated from the result of sorption measurement at 76 cmHg. Fig. 5(b) and (c) shows the plots of S and $\bar{D}$ for the blends, respectively. It

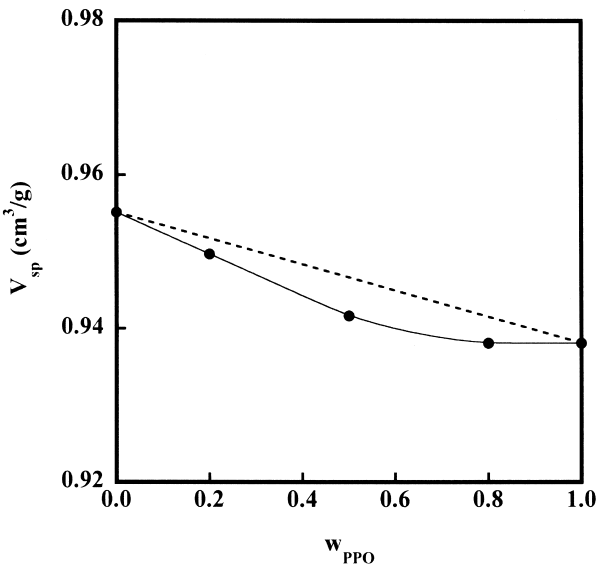

Fig. 2. Specific volume plotted against weight fraction of PPO in the blend at 25 °C.

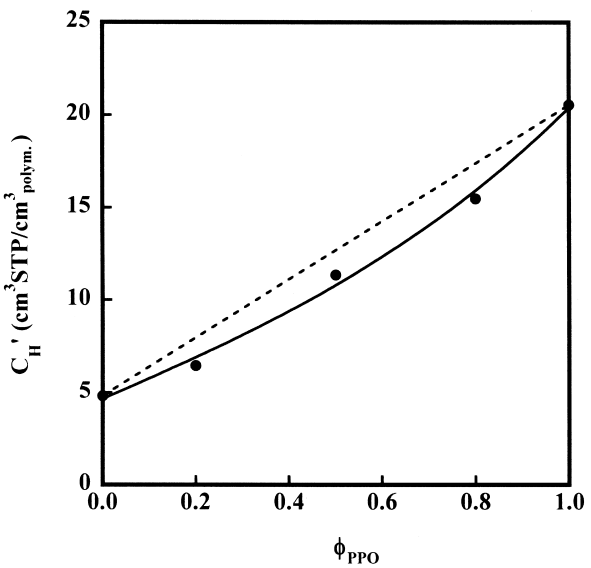

Fig. 4. Langmuir saturation constant of Xe plotted against volume fraction of PPO in the blend at 25 °C.

Table 1
Dual-mode sorption parameters of Xe at 25 °C and glass transition temperature (T_g) of PPO/PS blends

PPO/PS	C'_H (cm^3 STP/cm$^3_{polym.}$)	$k_D \times 10^2$ (cm^3 STP/cm$^3_{polym.}$ cmHg)	$b \times 10^3$ (cm Hg^{-1})	T_g (°C)
0/100	4.8	1.1	8.8	100
20/80	6.4	1.2	7.8	115
50/50	11.3	1.3	7.7	144
80/20	15.5	1.5	7.9	174
100/0	20.6	1.7	7.8	216

is found that the $\bar{D}$ shows a negative deviation from the additive rule as well as the $\bar{P}$, which is fundamentally consistent with CO_2 and CH_4 transport properties investigated by Maeda et al. [44]. On the other hand, the S follows the additive rule. This fact means that the decrease in the $\bar{P}$ for the blends is attributed to the decrease in the $\bar{D}$. In order to analyze the decrease in the diffusivity in detail, the partial immobilized model [3,45–47] was applied.

$$\bar{P} = k_D D_D \left[1 + \frac{FK}{1 + bp} \right] \tag{7}$$

$$F = \frac{D_H}{D_D} \tag{8}$$

$$K = \frac{C'_H b}{k_D} \tag{9}$$

D_D and D_H are diffusion coefficients of Xe for Henry and Langmuir sites, respectively. Fig. 6 shows plots of $\bar{P}$s of the blends against $1/(1 + bp)$ derived from the sorption measurement. The plots follow a fairly good linearity, which demonstrates the applicability of the partial immobilized model to Xe transport for the blends as well as other polymer–penetrant systems. The D_D and D_H can be obtained from intercept and slope of the plot shown in Fig. 6, respectively. Fig. 7 shows plots of D_D, D_H, and F against volume fraction of PPO in the blend. A negative deviation from a semilogarithmic additive rule of D_H is considerable in comparison with that of D_D, and, as a consequence, F shows a negative deviation. These results indicate that the decrease in the diffusivity of Xe in the blends is attributed to the decrease in that for the Langmuir site, which is correlated to the decrease in the total amount of microvoids by blending.

3.2. Characterization of microvoids by ^{129}Xe NMR spectroscopy

Fig. 8 shows ^{129}Xe NMR spectra of ^{129}Xe in PPO obtained at various pressures. It is recognized that the symmetric peak shifts to low magnetic field with increasing pressure of Xe, and similar results were obtained for others. These downfield shifts are caused by increase in the interaction between Xe atoms, that is, the contribution of term δ(Xe) in Eq. (2). Additionally the symmetric peak indicates that Xe atoms dissolved in a glassy polymer diffuse fast, and then exchange rapidly between the Henry and Langmuir sites in the NMR time scale. Fig. 9 shows the plots of ^{129}Xe NMR chemical shifts for the blends against sorption amount of C. It is confirmed that the NMR chemical shifts show non-linear low-field shift with increasing sorption amount of C. In general, ^{129}Xe NMR chemical shift shows linear low-field shift with increasing concentration of Xe, i.e. sorption amount of Xe. For example, the NMR chemical shift of ^{129}Xe in gas phase shifts to low-field linearly with increasing concentration of Xe, and, in many cases, the NMR chemical shifts of ^{129}Xe in zeolites that have no strong charges also shift linearly with increasing sorption amount of Xe. Since the sorption amount of C for a glassy polymer is composed of C_D and C_H (see Eq. (1)), which is a essential difference from the cases of ^{129}Xe in gas phase and zeolites, it is necessary to evaluate C_D and C_H dependences of ^{129}Xe NMR chemical

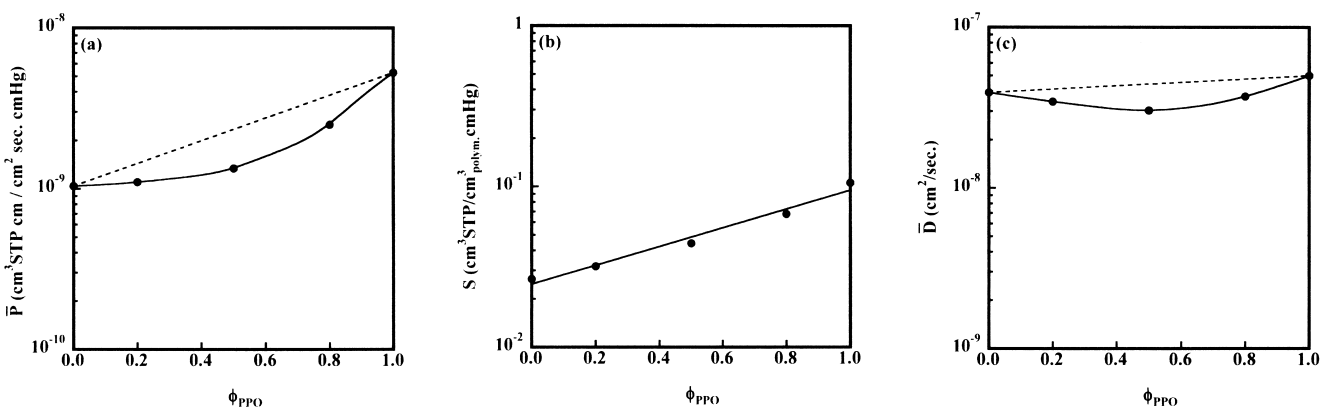

Fig. 5. Permeability (a), diffusion (b), and solubility (c) coefficients of Xe for PPO/PS blends plotted against volume fraction of PPO in the blend at 25 °C.

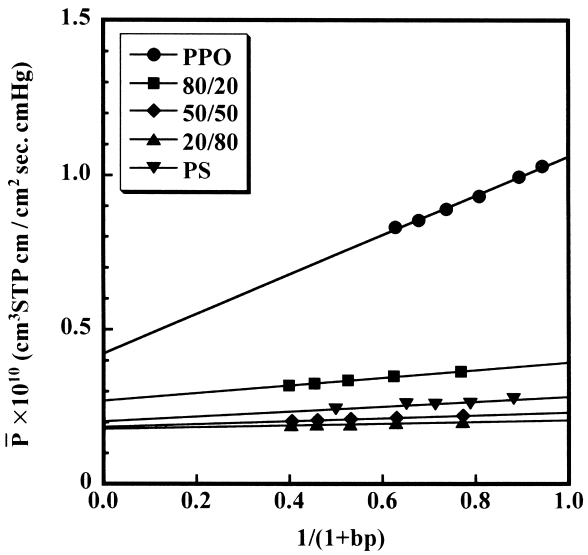

Fig. 6. Xe permeability coefficients plotted in accordance with the partial immobilized model for PPO/PS blends at 25 °C.

shifts individually. Assuming a fast exchange of Xe atoms between Henry and Langmuir sites [12,48], ^{129}Xe NMR chemical shifts for each site were calculated using the dual-mode sorption parameters of Xe summarized in Table 1:

$$\delta_{obs.} = f_D\delta_D + f_H\delta_H \tag{10}$$

$$f_D + f_H = \frac{C_D}{C} + \frac{C_H}{C} = 1 \tag{11}$$

where $\delta_{obs.}$ is the observed NMR chemical shift, f_D and f_H are fractional concentrations of Xe for the Henry and Langmuir sites at each pressure, and δ_D and δ_H are the NMR chemical shifts for Henry and Langmuir sites, respectively. For further equations, subscripts D and H correspond to the Henry and Langmuir sites, respectively. From Eq. (2), NMR chemical shifts for each site are explained by following

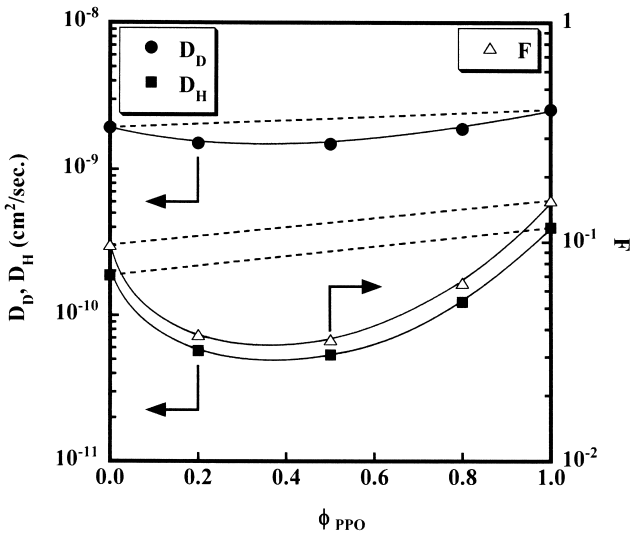

Fig. 7. Plots of D_D, D_H, and F against volume fraction of PPO in the blend.

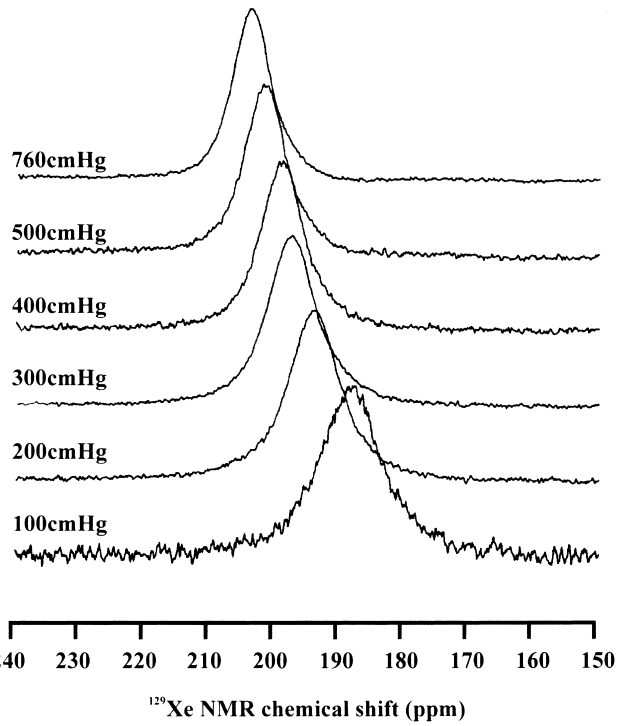

Fig. 8. ^{129}Xe NMR spectra of ^{129}Xe sorbed in PPO under various pressures of Xe at 25 °C.

equations:

$$\delta_D = \delta(Xe)_D + \delta(S)_D = A_D C_D + \delta(S)_D \tag{12}$$

$$\delta_H = \delta(Xe)_H + \delta(S)_H = A_H C_H + \delta(S)_H \tag{13}$$

where A_i is the constant, C_i is the sorption amount of Xe, and $\delta(S)_i$ is the NMR chemical shift due to the interaction between Xe and inner wall of hole. Using Eqs. (1) and (10)–(13), concentration dependences of the NMR chemical shifts for each site were calculated (Fig. 10). It should be

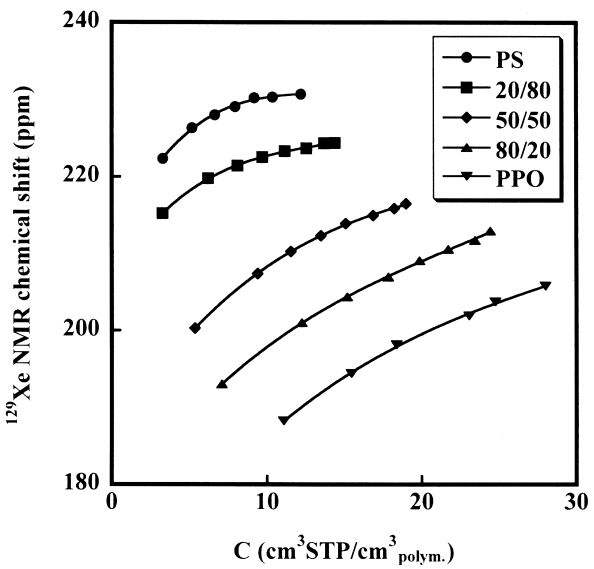

Fig. 9. ^{129}Xe NMR chemical shifts plotted against sorption amount of Xe for PPO/PS blends at 25 °C.

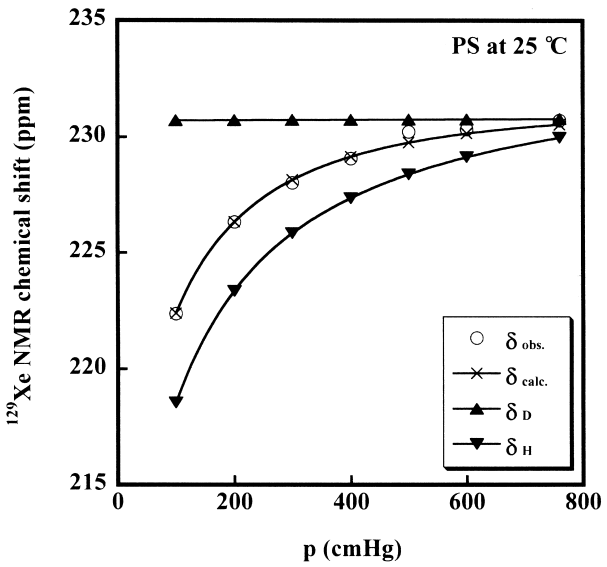

Fig. 10. ^{129}Xe NMR chemical shifts of ^{129}Xe sorbed in PS plotted against pressure of Xe at 25 °C.

noted that the unit of the horizontal axis in Fig. 10 is the pressure (cmHg). It turns out that δ_D reveals lower field than $\delta_{obs.}$, and δ_H reveals opposite. The parameters in Eqs. (12) and (13) are summarized in Table 2. It proves that A_H is larger than A_D about one order of magnitude for individual membranes, which indicates that the concentration dependence of the NMR chemical shift for the Langmuir site is larger than that for the Henry site. In practice, for a rubbery polymer that contains only Henry site, the NMR chemical shift hardly depends on the concentration of Xe (data not shown), suggesting the inhibition of the interaction between Xe atoms by mobile molecular chains. In a similar manner, for a glassy polymer, it can be thought local molecular motions around part of main chains and/or side chains that may provide the Henry-mode sorption site inhibit the interaction between Xe atoms. On the other hand, since there are no inhibitory factors in the Langmuir-mode sorption site, that is, microvoids, A_H becomes larger than A_D. Moreover f_H is higher than f_D at low-pressure region, while that is opposite at high-pressure region. For these reasons, the NMR chemical shift of ^{129}Xe sorbed in a glassy polymer apparently shows non-linear low-field shift against total sorption amount of C as shown in Fig. 9.

It can be said that the NMR chemical shift extrapolated to $C_H = 0$ for the δ_H, that is, $\delta(S)_H$ in Eq. (13) reflects the mean size of microvoids. According to Fraissard and co-workers, when the NMR chemical shift of ^{129}Xe in zeolites is determined only by the interaction between Xe and inner wall of hole, and also the contributions of terms δ(E), δ(SAS), and δ(M) are absent or quite negligible, the mean free path λ can be linked to δ(S) in Eq. (2). Hence the mean size of microvoids in a glassy polymer can likewise be estimated by following relation [11–12]:

$$\delta(S)_H = 243 \times \frac{2.054}{2.054 + \lambda} \tag{14}$$

where λ is a function of both hole shape and hole dimension. When the shape of microvoids in a glassy polymer is assumed to be spherical, the following relation is derived:

$$\lambda = \frac{(d_S - d_{Xe})}{2} \tag{15}$$

where d_S is the diameter of the sphere and d_{Xe} is the van der Waals diameter of Xe atom = 4.4 Å. Table 3 lists the obtained values of $\delta(S)_H$ and d_S for the blends. It appears that mean sizes of microvoids are in the order of angstrom. From d_S, the mean volume of individual microvoids, v (cm^3), is calculated:

$$v = \frac{4\pi[(d_S/2) \times 10^{-8})]^3}{3} \tag{16}$$

Furthermore C'_H should be expressed by the product of mean volume and number of microvoids since C'_H is the indicator of total amount of microvoids in a glassy polymer. Thus the parameter N correlated with the number of microvoids in a glassy polymer can be defined by following equation:

$$N = \frac{C'_H}{v} \tag{17}$$

Fig. 11 shows the plots of v and N against volume fraction of PPO in the blend. It appears that v values for the blends are smaller than those predicted by an additive rule, whereas N values vary in proportional to the volume fraction of PPO. This fact indicates that decrease in the total amount of microvoids is attributed not to decrease in the number of microvoids but to contraction of individual microvoids. In addition, it is elucidated that the contraction of microvoids highly affects gas transport properties of PPO/PS blends.

Table 2
Parameters of ^{129}Xe NMR chemical shifts for PPO/PS blends

PPO/PS	A_D (ppm cm$^3_{polym.}$/cm^3 STP)	$\delta(S)_D$ (ppm)	A_H (ppm cm$^3_{polym.}$/cm^3 STP)	$\delta(S)_H$ (ppm)
0/100	0.012	230.8	5.8	205.4
20/80	0.17	225.0	3.1	203.9
50/50	0.36	220.3	2.0	189.6
80/20	0.55	217.9	1.9	176.5
100/0	0.64	205.0	1.8	168.3

Table 3
$\delta(S)_H$ and d_S for PPO/PS blends

PPO/PS	$\delta(S)_H$ (ppm)	d_S (Å)
0/100	205.4	5.1
20/80	203.9	5.2
50/50	189.6	5.6
80/20	176.5	6.0
100/0	168.3	6.2

4. Conclusions

In this study, relationships among variations of microvoids and gas transport properties for miscible PPO/PS blends have been investigated by Xe sorption, Xe permeation, and ^{129}Xe NMR measurements. Langmuir saturation constants of Xe for the blends are smaller than those expected from an additive rule owing to the decrease in total amount of microvoids by blending. Decrease in the permeability of Xe is attributed to the decrease in the diffusivity of that in the Langmuir site. ^{129}Xe NMR spectra of ^{129}Xe sorbed in the blends obtained at various pressures show non-linear low-field shift because of a fast exchange of Xe between Henry and Langmuir sites. This behavior is one of the noticeable features for glassy polymers in comparison with many cases of rubbery polymers and zeolites. From the analysis of $\delta(S)_H$, which is the NMR chemical shift reflecting the mean size of microvoids, it can be demonstrated that mean volume of individual microvoids varies non-linearly from 71 Å^3 for PS to 126 Å^3 for PPO against volume fraction of PPO in the blend, which indicates the contraction of microvoids by blending. For PPO/PS blends, it is concluded that the contraction of microvoids occurs by blending and highly affects gas transport properties.

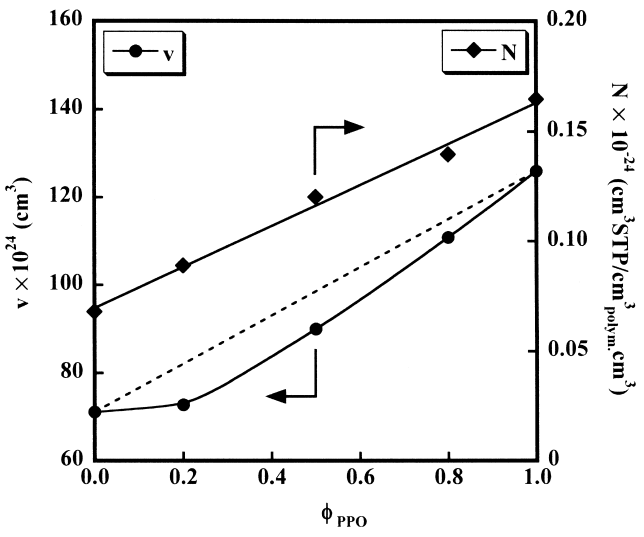

Fig. 11. Plots of v and N against volume fraction of PPO in the blend.

Acknowledgements

We gratefully acknowledge partial financial supports by a Grant-in-Aid for Scientific Research on Priority Areas (B), No. 13133202 (2001) from the Ministry of Education, Culture, Sports, Science and Technology (Japan), and Mukai Science and Technology Foundation.

References

[1] Chan AH, Paul DR. J Appl Polym Sci 1979;24:1539–50.
[2] Tsujita Y, Hachisuka H, Imai T, Takizawa A, Kinoshita T. J Membr Sci 1991;60:103–11.
[3] Koros WJ, Paul DR. J Polym Sci, Polym Phys Ed 1978;16:2127–87.
[4] Hachisuka H, Tsujita Y, Takizawa A, Kinoshita T. Polymer 1988;29:2050–5.
[5] Hachisuka H, Tsujita Y, Takizawa A, Kinoshita T. Polym J 1989;21:1019–25.
[6] Nagai K, Toy LG, Freeman BD, Teraguchi M, Masuda T, Pinnau I. J Polym Sci B Polym Phys 2000;38:1474–84.
[7] Nakagawa T, Watanabe T, Mori M, Nagai K. In: Freeman BD, Pinnau I, editors. Polymer membranes for gas and vapor separation. ACS Symposium Series No. 733, Washington, DC: American Chemical Society; 1999. p. 68–84.
[8] Koros WJ, Smith GN, Stannett V. J Appl Polym Sci 1981;26:159–70.
[9] Muruganandam N, Koros WJ, Paul DR. J Polym Sci B Polym Phys 1987;25:1999–2026.
[10] Pinnau I, Casillas CG, Morisato A, Freeman BD. J Polym Sci B Polym Phys 1997;35:1483–90.
[11] Demarquay J, Fraissard J. Chem Phys Lett 1987;136:314–8.
[12] Fraissard J, Ito T. Zeolites 1988;8:350–61.
[13] Ito T, Fraissard J. Zeolites 1987;7:554–8.
[14] Barrie PJ, Klinowski J. Prog NMR Spectrosc 1992;24:91–108.
[15] Ito T, Fraissard J. J Chem Soc, Faraday Trans 1 1987;83:451–62.
[16] Gédéon A, Bonardet JL, Lepetit C, Fraissard J. Solid State Nucl Magn Reson 1995;5:201–12.
[17] Springuel-Huet MA, Bonardet JL, Gédéon A, Fraissard J. Magn Reson Chem 1999;37:S1–S13.
[18] Ito T, De Menorval LC, Guerrier E, Fraissard JP. Chem Phys Lett 1984;111:271–4.
[19] Ripmeester JA, Ratcliffe CI, Tse JS. J Chem Soc, Faraday Trans 1988;84:3731–45.
[20] Ito T, Springuel-Huet MA, Fraissard J. Zeolites 1989;9:68–73.
[21] Fetter G, Tichit D, De Ménorval LC, Fraissard J. Appl Catal 1990;65:L1–L4.
[22] Walton JH, Miller JB, Roland CM. J Polym Sci B Polym Phys 1992;30:527–32.
[23] Walton JH, Miller JB, Roland CM. Macromolecules 1993;26:5602–10.
[24] Jokisaari J. Prog NMR Spectrosc 1994;26:1–26.
[25] Miyoshi T, Takegoshi K, Terao T. Polymer 1997;38:5475–80.
[26] Schantz S, Veeman WS. J Polym Sci B Polym Phys 1997;35:2681–8.
[27] Wang Y, Inglefield PT, Jones AA. Polymer 2002;43:1867–72.
[28] Wang Y, Inglefield PT, Jones AA. J Polym Sci B Polym Phys 2002;40:1965–74.
[29] Suzuki T, Miyauchi M, Yoshimizu H, Tsujita Y. Polym J 2001;33:934–8.
[30] Suzuki T, Miyauchi M, Takekawa M, Yoshimizu H, Tsujita Y, Kinoshita T. Macromolecules 2001;34:3805–7.
[31] Suzuki T, Yoshimizu H, Tsujita Y. Desalination 2002;148:359–61.
[32] Hill AJ, Jones PL, Lind JH, Pearsall GW. J Polym Sci, Part A: Polym Chem 1988;26:1541–52.

[33] Ruan MY, Moaddel H, Jamieson AM, Simha R, McGervey JD. Macromolecules 1992;25:2407–11.
[34] Liu J, Jean YC, Yang H. Macromolecules 1995;28:5774–9.
[35] Bartoš J, Krištiaková K, Šauša O, Krištiak J. Polymer 1996;37: 3397–403.
[36] Li HL, Ujihira Y, Nanasawa A, Jean YC. Polymer 1999;40:349–55.
[37] Hagiwara K, Ougizawa T, Inoue T, Hirata K, Kobayashi Y. Radiat Phys Chem 2000;58:525–30.
[38] Bohlen J, Kirchheim R. Macromolecules 2001;34:4210–5.
[39] Djordjevic MB, Porter RS. Polym Engng Sci 1983;23:650–7.
[40] Weinkauf DH, Kim HD, Paul DR. Macromolecules 1992;25:788–96.
[41] Morisato A, Shen HC, Sankar SS, Freeman BD, Pinnau I, Casillas CG. J Polym Sci B Polym Phys 1996;34:2209–22.
[42] Pinnau I, Casillas CG, Morisato A, Freeman BD. J Polym Sci B Polym Phys 1996;34:2613–21.
[43] Dixon-Garrett SV, Nagai K, Freeman BD. J Polym Sci B Polym Phys 2000;38:1078–89.
[44] Maeda Y, Paul DR. Polymer 1985;26:2055–63.
[45] Paul DR, Koros WJ. J Polym Sci, Polym Phys Ed 1976;14:675–85.
[46] Koros WJ, Paul DR, Rocha AA. J Polym Sci, Polym Phys Ed 1976;14: 687–702.
[47] Merkel TC, Bondar V, Nagai K, Freeman BD. J Polym Sci B Polym Phys 2000;38:273–96.
[48] Rittner F, Seidel A, Sprang T, Boddenberg B. Appl Spectrosc 1996; 50:1389–94.